Thomas and Fromme, https://doi.org/10.1083/jcb.201608123

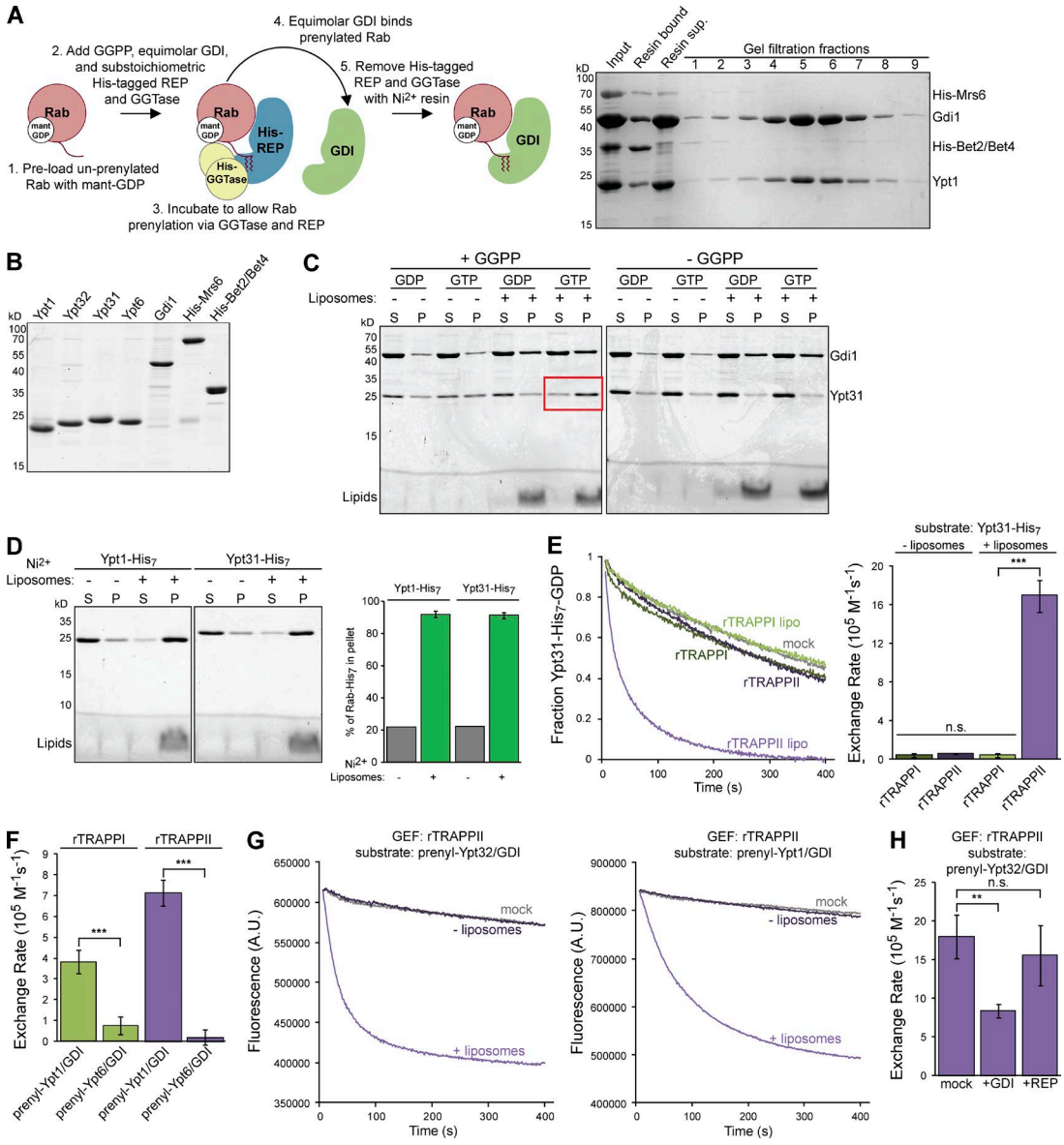

Figure S1. **Generation of prenylated-Rab/GDI complexes and GEF activity assay controls.** (A, left) Schematic depicting the workflow used to generate prenylated-Rab/GDI complexes used as substrates in GEF activity assays. Consistent with proposed mechanisms of Rab prenylation (Goody et al., 2005), we found that the REP Mrs6 was required for geranylgeranylation of the Rab C-terminal cysteines. We therefore used substoichiometric concentrations of the REP and the geranylgeranyl transferase (GGTase) Bet2/Bet4 to generate the desired prenylated-Rab/GDI complexes. (right) Example of samples taken during a Ypt1 prenylation reaction. Gel-filtration fractions 4, 5, and 6 with stoichiometric prenylated-Ypt1/GDI complexes were pooled and used as substrates in GEF assays. (B) 0.5 µg of each reagent used to generate prenylated-Rab/GDI complexes were run on a 15% SDS-PAGE gel and stained for total protein. (C) Liposome pelleting assays with Ypt31/GDI complexes prepared with and without GGPP. Ypt31/GDI complexes were assayed for membrane binding after exchange with GDP or GTP. Rabs from complexes prepared with GGPP shed their GDI and bind membranes in a nucleotide-dependent manner (red box). (D) Liposome pelleting assays with similar conditions as used in GEF assays showing that >90% of His-tagged Rabs are membrane-anchored in GEF assays. Error bars represent 95% CIs of $n = 2$ independent experiments. (E, left) Normalized representative traces showing activation of His-tagged Ypt31 by rTRAPPI or II in the presence or absence of TGN liposomes (lipo). "mock" is a control lacking TRAPP for intrinsic exchange of His-tagged Rabs. (right) Rates of TRAPP-mediated Ypt31-His_7 activation determined from the traces at left. Error bars represent 95% CIs for $n \geq 2$ reactions (without liposomes) or $n \geq 3$ reactions (with liposomes). (F) Rates of prenylated-Ypt1/GDI and prenylated-Ypt6/GDI activation by rTRAPPI and -II in the presence of TGN liposomes. Error bars represent 95% CIs for $n = 3$ reactions. (G) Representative fluorescence traces showing a lack of activation of prenylated Rabs by rTRAPPII in the absence of liposome membranes. Traces are representative of $n > 5$ independent experiments. (H) Rates of prenylated-Ypt32/GDI activation by rTRAPPII on TGN liposomes in the absence (mock) or presence of a fivefold molar excess of GDI or REP. Error bars represent 95% CIs for $n \geq 3$ reactions. A.U., arbitrary units; P, membrane pellet; S, supernatant. n.s., not significant; **, $P < 0.01$; **, $P < 0.001$.

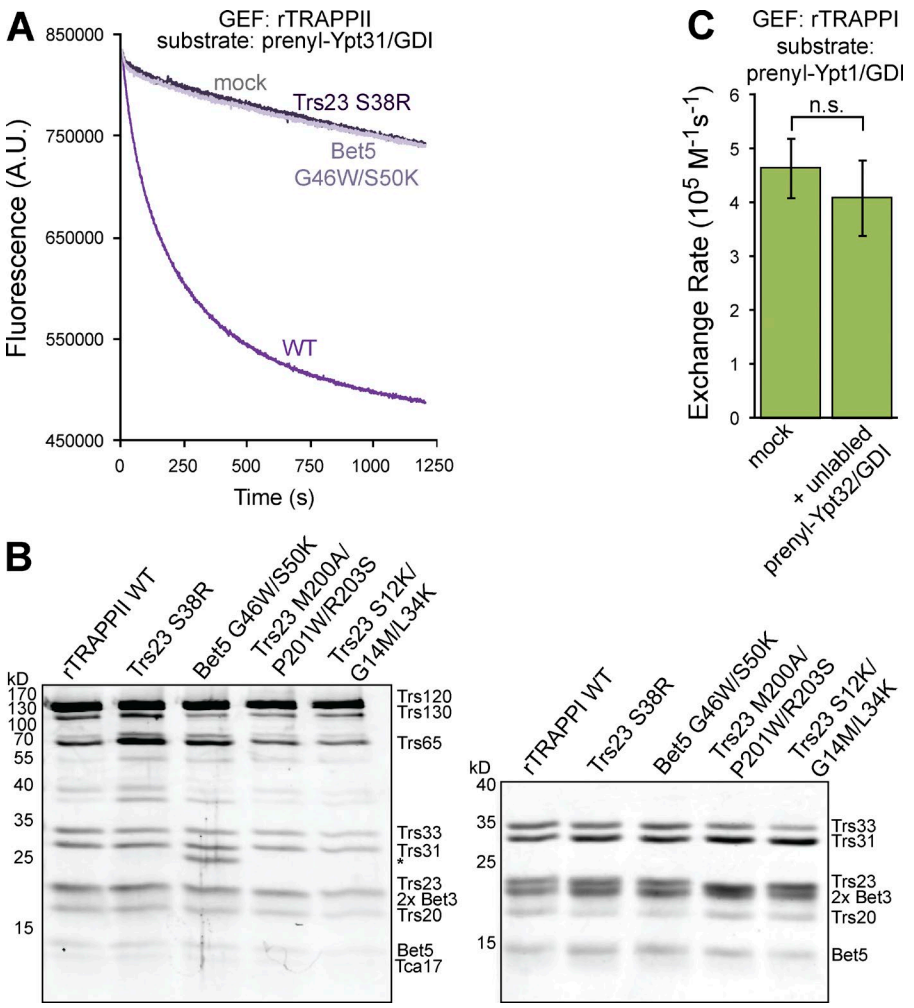

Figure S2. **Catalytic site mutants do not affect TRAPP complex assembly.** (A) Representative fluorescence traces showing a lack of activation of prenylated-Ypt31/GDI on TGN liposomes by the indicated rTRAPPII active site mutants. Ypt31 was not activated by the rTRAPPII mutants tested, and exponential functions could not be fit to experimental curves. Traces are representative of $n \geq 3$ independent experiments. (B, left) rTRAPPII mutant complexes were purified via Trs130-TAP. Asterisk indicates contaminant. (right) rTRAPPI mutant complexes were purified via His_6-Trs31. (C) rTRAPPI-mediated activation of mantGDP-labeled prenylated-Ypt1/GDI on TGN liposomes in the absence (mock) or presence of equimolar concentrations of competing unlabeled prenylated-Ypt32/GDI. Error bars represent 95% CIs for $n = 3$ reactions. A.U., arbitrary units. n.s., not significant.

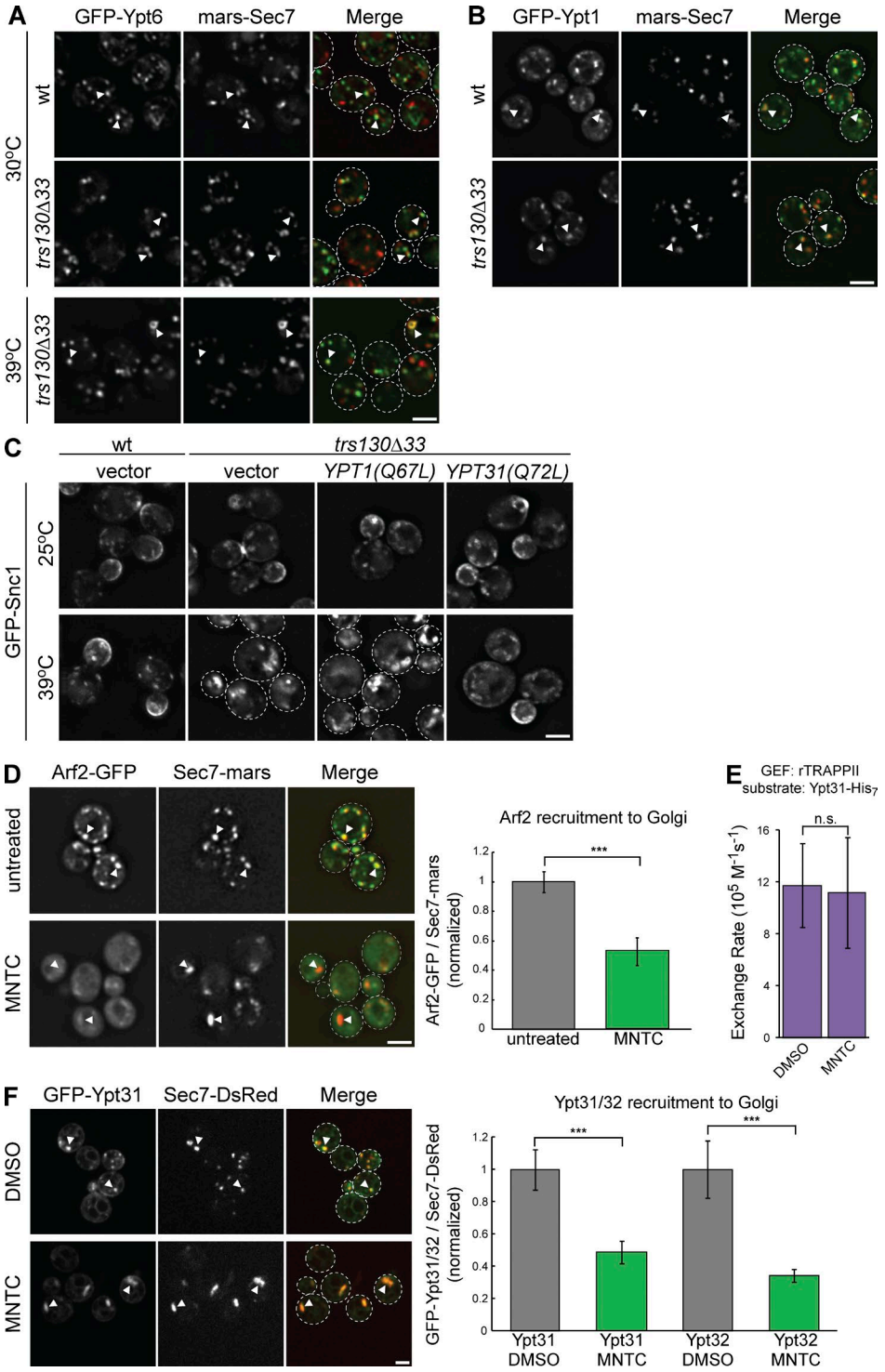

Figure S3. **Ypt31 overexpression restores trafficking in a TRAPPII mutant, and MNTC inhibits Arf1 activation and Ypt31/32 recruitment in vivo.** (A) Localization of plasmid-borne GFP-Ypt6 relative to mRFPmars-Sec7 in WT versus *trs130Δ33* yeast grown at the permissive temperature or after shifting to the restrictive temperature for 60 min. (B) Localization of plasmid-borne GFP-Ypt1 relative to the late Golgi marker mRFPmars-Sec7 in WT versus *trs130Δ33* yeast grown at the permissive temperature (30°C). (C) Localization of GFP-Snc1, a SNARE that cycles among the late Golgi, plasma membrane, and endocytic vesicles, in WT versus *trs130Δ33* yeast grown at the permissive temperature or after shifting to the restrictive temperature for 60 min. Constitutively active Ypt1(Q67L) and Ypt31(Q72L) were overexpressed on high-copy plasmids to test their ability to rescue Snc1 transport in the temperature-sensitive *trs130Δ33* yeast. (D, left) Localization of Arf2-GFP relative to Sec7-mRFPmars in cells treated with or without MNTC for 20 min. (right) Recruitment of Arf2 to Golgi compartments was measured by quantifying the ratio of Arf2-GFP to Sec7-mRFPmars in Sec7-mRFPmars puncta. Error bars represent 95% CIs for $n = 66$ (untreated) or $n = 21$ (MNTC-treated) Golgi compartments. (E) Rates of Ypt31-His_7 activation by rTRAPPII on TGN liposomes in the presence of DMSO (vehicle control) or MNTC. Error bars represent 95% CIs for $n = 3$ reactions. (F, left) Localization of GFP-Ypt31 relative to Sec7-6xDsRed in cells treated with DMSO or MNTC for 10 min. (right) Recruitment of Ypt31/32 to Golgi compartments was measured as in A. Error bars represent 95% CIs for $n \geq 40$ Golgi compartments. Bars, 2 µm. White arrowheads denote colocalization of GFP-tagged GTPases with Sec7 at Golgi compartments. n.s., not significant; ***, $P < 0.001$.

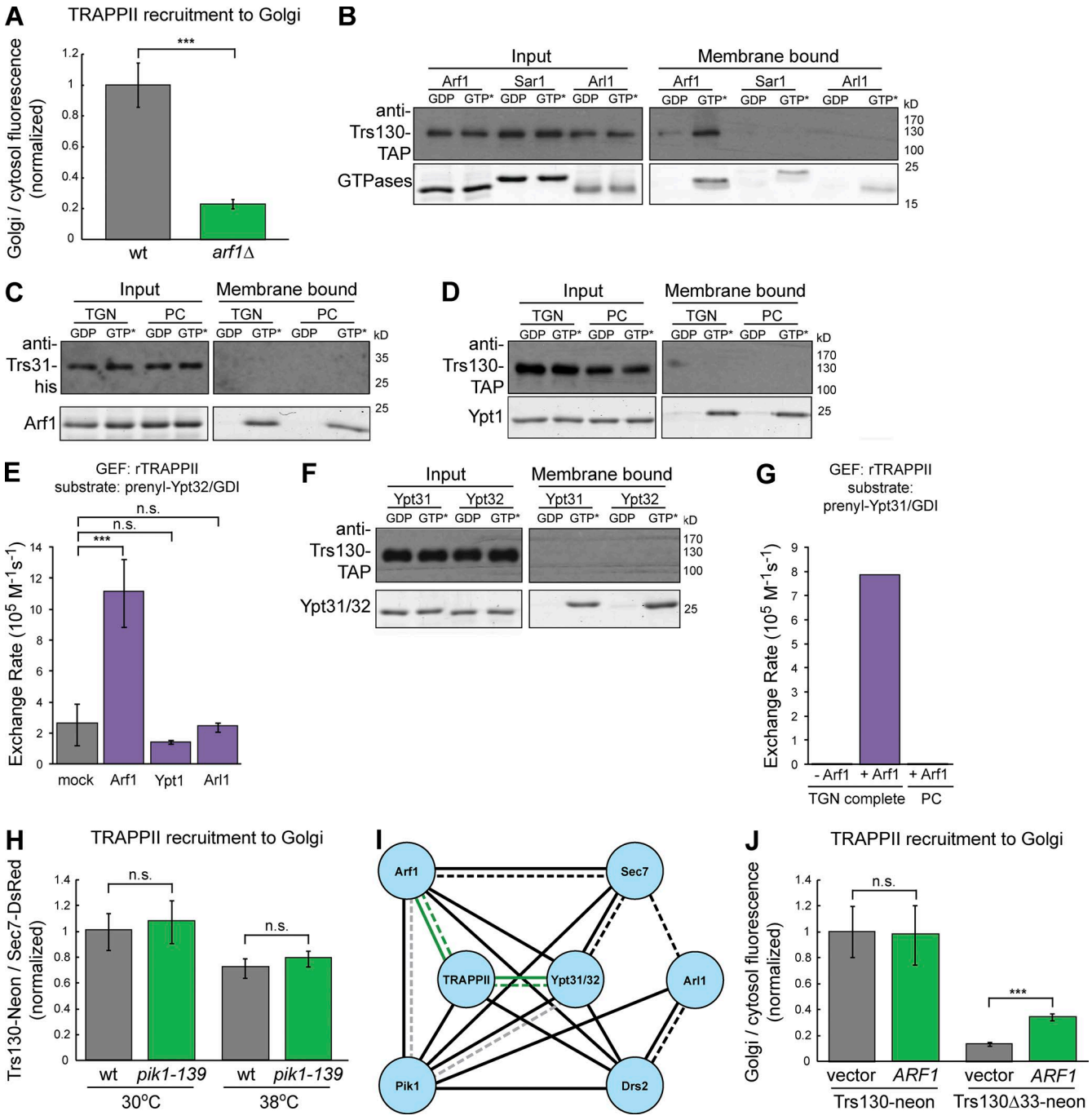

Figure S4. **TRAPPII membrane-recruitment controls.** (A) Line-trace quantification of cytosolic and Golgi localization of TRAPPII in WT versus *arf1Δ* yeast grown at 30°C. Error bars represent 95% CIs for $n \geq 10$ cells. (B) Liposome flotation showing that activated myristoylated-Arf1, but not Sar1 or Arl1, recruits rTRAPPII to TGN liposomes. Liposomes do not contain Ni^{2+}-DOGS (See Materials and methods). (C) Liposome flotation showing that activated myristoylated-Arf1 does not recruit rTRAPPI to TGN or PC liposomes. Liposomes do not contain Ni^{2+}-DOGS. (D) Liposome flotation showing that activated prenylated-Ypt1 does not recruit rTRAPPII to TGN or PC liposomes. Liposomes do not contain Ni^{2+}-DOGS. (E) Rates of rTRAPPII-catalyzed prenylated-Ypt32/GDI activation on TGN liposomes in the absence (mock) or presence of activated myristoylated-Arf1, prenylated-Ypt1, or myristoylated-Arl1. Liposomes do not contain Ni^{2+}-DOGS. Error bars represent 95% CIs for $n \geq 2$ reactions. (F) Liposome flotation showing that activated prenylated-Ypt31/32 does not recruit rTRAPPII to TGN liposomes. Liposomes do not contain Ni^{2+}-DOGS. (G) Rates of rTRAPPII-catalyzed prenylated-Ypt31/GDI activation on TGN or PC liposomes in the presence and absence of activated myristoylated-Arf1. Liposomes do not contain Ni^{2+}-DOGS. Rates are representative of $n > 5$ independent experiments. (H) Recruitment of TRAPPII to Golgi compartments in WT versus *pik1-139* temperature-sensitive cells at the permissive temperature or after shifting the restrictive temperature for 60 min. Recruitment was measured by quantifying the ratio of Trs130-mNeonGreen to Sec7-6xDsRed in Sec7-6xDsRed puncta. Error bars represent 95% CIs for $n \geq 43$ compartments. (I) Genetic (synthetic sick or lethal) and physical interactions among trafficking regulators at the late Golgi. Genetic and physical interactions are denoted by continuous and dashed lines, respectively. Interactions identified or reproduced in this study are indicated in green. Interactions reported in mammalian cells are represented in gray. (J) Line-trace quantification of cytosolic and Golgi localization of Trs130-mNeonGreen versus Trs130Δ33-mNeonGreen in WT cells with or without overexpression of Arf1. Error bars represent 95% CIs of $n \geq 10$ cells. GTP*, GMP-PNP. n.s., not significant; ***, $P < 0.001$.

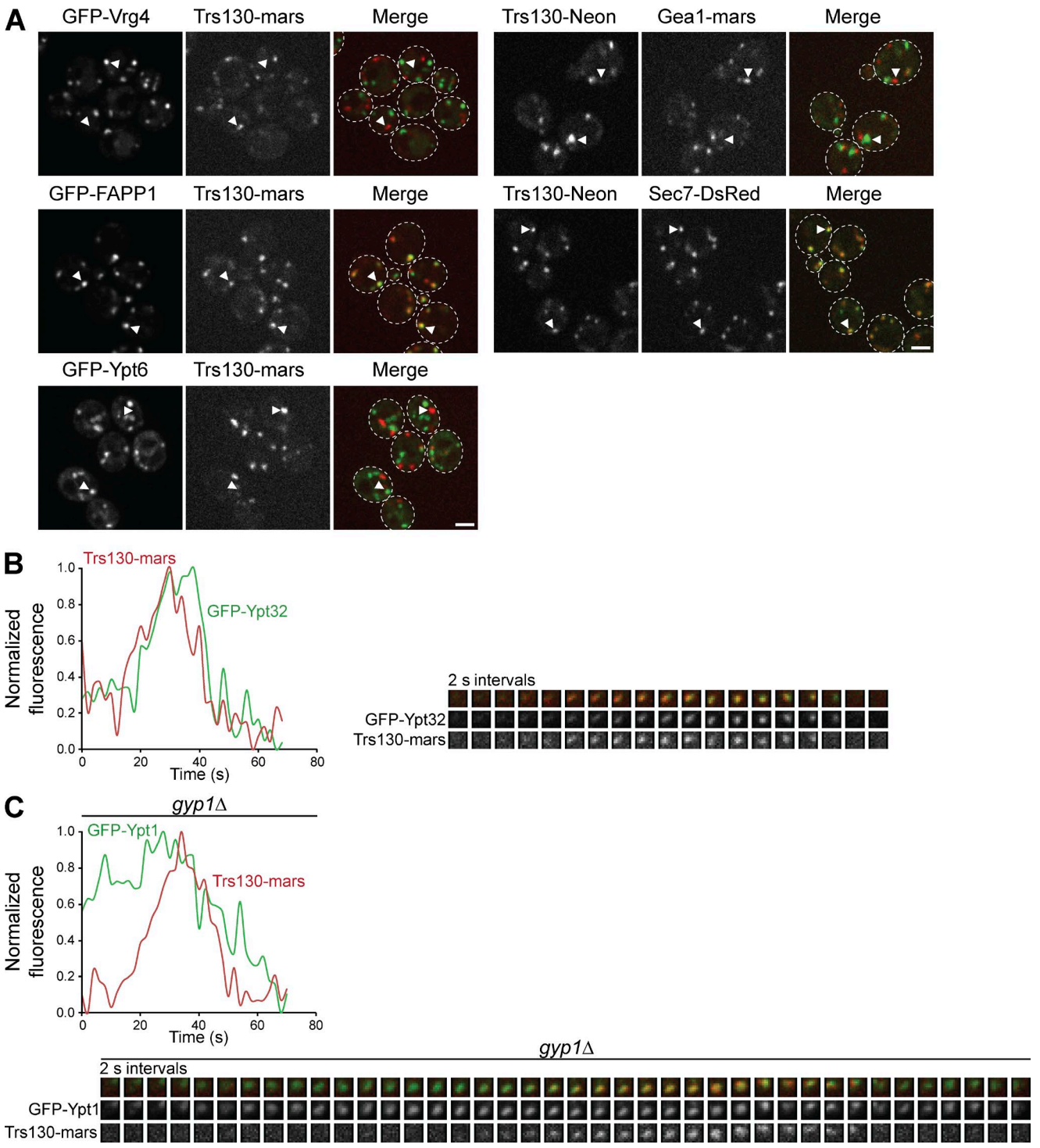

Figure S5. **TRAPPII does not localize to the early Golgi but overlaps with Ypt1 in *gyp1Δ* cells.** (A, left) Localization of Trs130-3xmRFPmars relative to the early Golgi marker GFP-Vrg4, GFP-hFAPP1 PH domain, a coincidence detector of PI(4)P and Arf1, and plasmid-borne GFP-Ypt6. (right) Localization of Trs130-mNeonGreen relative to the Arf1-GEFs Gea1-3xmRFPmars (early Golgi) and Sec7-6xDsRed (late Golgi/TGN). Bars, 2 µm. (B) Time-lapse imaging series (2-s intervals) and normalized quantification of GFP-Ypt32 and Trs130-3xmRFPmars at a single Golgi compartment. (C) Time-lapse imaging series (2-s intervals) and normalized quantification of GFP-Ypt1 and Trs130-3xmRFPmars at a single Golgi compartment in a *gyp1Δ* mutant. Regions of interest for time-lapse imaging series are 0.7 × 0.7 µm. White arrowheads denote colocalization, or not, of early and late Golgi markers with TRAPPII at Golgi compartments.

Table S1. **Plasmids used in this study**

Name	Description	Vector backbone	Source
Ypt1-His_7	Ypt1 with C-terminal His_7 tag and cleavable N-terminal GST tag	pGEX-6P	McDonold and Fromme, 2014
Ypt32-His_7	Ypt32 with C-terminal His_7 tag and cleavable N-terminal GST tag	pGEX-6P	A. Bretscher (Cornell University, Ithaca, NY)
pCM15	Ypt31 with C-terminal His_7 tag and cleavable N-terminal GST tag	pGEX-6P	McDonold and Fromme, 2014
pLT22	Vps21 with C-terminal His_7 tag and cleavable N-terminal GST tag	pGEX-6P	This study
pLT23	Sec4 with C-terminal His_7 tag and cleavable N-terminal GST tag	pGEX-6P	This study
pCM14	Ypt6 with C-terminal His_7 tag and cleavable N-terminal GST tag	pGEX-6P	McDonold and Fromme, 2014
pLT50	Full-length Ypt1 with cleavable N-terminal GST tag	pGEX-6P	This study
pLT81	Full-length Ypt32 with cleavable N-terminal GST tag	pGEX-6P	This study
pLT72	Full-length Ypt31 with cleavable N-terminal GST tag	pGEX-6P	This study
pLT82	Full-length Ypt6 with cleavable N-terminal GST tag	pGEX-6P	This study
pLT40	Gdi1 with cleavable N-terminal GST tag	pGEX-6P	This study
pLT35	Mrs6 with cleavable N-terminal His_6 tag	pET28	This study
pLT41	Bet2 with cleavable N-terminal His_6 tag and Bet4	pCDF-Duet-1	This study
pLT14	rTRAPPI with Trs33, His_6(TEV)Trs31, Trs23, Bet3, Trs20 and Bet5	pCOLA-Duet-1	This study
pLT21	rTRAPPI plasmid with His_6 tag removed from Trs31	pCOLA-Duet-1	This study
pLT16	Trs120 with cleavable N-terminal His_6 tag and Tca17	pET-Duet-1	This study
pLT36	Trs130 with C-terminal TAP tag and Trs65	pCDF-Duet-1	This study
pLT24	rTRAPPI with active site mutant Trs23 S38R	pCOLA-Duet-1	This study
pLT25	rTRAPPI (no His_6 tag) with active site mutant Trs23 S38R	pCOLA-Duet-1	This study
pLT27	rTRAPPI with active site mutant Bet5 G46W/S50K	pCOLA-Duet-1	This study
pLT28	rTRAPPI (no His_6 tag) with active site mutant Bet5 G46W/S50K	pCOLA-Duet-1	This study
pLT67	rTRAPPI with active site mutant Trs23 M200A/P201W/R203S	pCOLA-Duet-1	This study
pLT66	rTRAPPI (no His_6 tag) with active site mutant Trs23 M200A/P201W/R203S	pCOLA-Duet-1	This study
pLT64	rTRAPPI with active site mutant Trs23 S12K/G14M/L34K	pCOLA-Duet-1	This study
pLT61	rTRAPPI (no His_6 tag) with active site mutant Trs23 S12K/G14M/L34K	pCOLA-Duet-1	This study
pNmt1	Nmt1	pCYC	Duronio et al., 1990
pArf1	Arf1	pET3c	Weiss et al.,1989
pCF1184	Arl1	pET23	McDonold and Fromme, 2014
pRS425	Yeast 2-µm vector with *LEU2* marker	pRS425	Sikorski and Hieter, 1989
pRS416	Yeast centromeric vector with *URA3* marker	pRS416	Sikorski and Hieter, 1989
pLT31	*YPT1* gene in pRS425	pRS425	This study
pLT32	*YPT1(Q67L)* GTP-locked mutant in pRS425	pRS425	This study
VBS327	*YPT31* gene in pRS425	pRS425	Sciorra et al., 2005
VBS333	*YPT31(Q72L)* GTP-locked mutant in pRS425	pRS425	Sciorra et al., 2005
pCF1022	*ARF1* gene in pRS416	pRS416	This study
pLT86	*ARF1(Q71L)* GTP-locked mutant in pRS416	pRS416	This study
pLT45	mRFPmars-Sec7 in pRS415	pRS415	This study
pLT44	mRFPmars-Sec7 in pRS416	pRS416	This study
pRC2100	GFP-Ypt1 in pRS415	pRS415	Buvelot Frei et al., 2006
pRC650	GFP-Ypt6 in pRS415	pRS415	Buvelot Frei et al., 2006
pRC678	GFP-Ypt31 integration plasmid	pRS306	Buvelot Frei et al., 2006
pRC679	GFP-Ypt32 integration plasmid	pRS306	Buvelot Frei et al., 2006
APB2661	GFP-Snc1 integration plasmid	pRS306	Lewis et al., 2000
Sec7-6xDsRed	Sec7-6xDsRed integration plasmid	pRS406	Losev et al., 2006
iGFP-Vrg4	iGFP-Vrg4 integration plasmid	YIplac211	B. Glick (University of Chicago, Chicago, IL)
GFP-FAPP1	GFP-hFAPP1 PH domain integration plasmid	pRS406	Levine and Munro, 2002

Table S2. **Yeast strains used in this study**

Name	Description	Source
SEY6210	*MATα ura3-52 his3-Δ200 leu2-3,112 lys2-801 trp1-Δ901 suc2-Δ9*	Robinson et al., 1988
SEY6210.1	*MATa ura3-52 his3-Δ200 leu2-3,112 lys2-801 trp1-Δ901 suc2-Δ9*	Robinson et al., 1988
BY4741α	*MATα ura3-Δ0 his3-Δ1 leu2-Δ0 lys2-Δ0*	Brachmann et al., 1998
RSY298	*MATa trp1-1 his3-11,15 leu2-3,112 can1-100 ura3-1 ade2-1 sec7-1*	Esmon et al., 1981
CFY1205	SEY6210 *Arf2-GFP::HIS3 Sec7-mRFPmars::TRP1*	This study
CFY1805	SEY6210 *GFP-Ypt31::URA3 Sec7-6xDsRed::URA3::ura3*	McDonold and Fromme, 2014
CFY1806	*SEY6210 ura3::GFP-Ypt32::URA3 Sec7-6xDsRed::URA3::ura3*	McDonold and Fromme, 2014
CFY1903	*MATa his3-Δ1 leu2-Δ0 met15-Δ0 ura3-Δ0 Trs120-TAP::HIS3*	GE Healthcare
CFY2156	SEY6210.1 *trs130Δ33::KanMX*	This study
CFY2223	SEY6210.1 *GFP-Snc1::URA3*	This study
CFY2225	SEY6210.1 *trs130Δ33::KanMX GFP-Snc1::URA3*	This study
CFY2297	SEY6210.1 *GFP-Ypt31::URA3*	This study
CFY2299	SEY6210.1 *GFP-Ypt31::URA3 trs130Δ33::KanMX*	This study
CFY2301	SEY6210.1 *GFP-Ypt32::URA3*	This study
CFY2303	SEY6210.1 *GFP-Ypt32::URA3 trs130Δ33::KanMX*	This study
CFY2451	SEY6210.1 *Trs130-mNeonGreen::HIS3*	This study
CFY2454	SEY6210.1 *Trs130Δ33-mNeonGreen::HIS3*	This study
CFY2545	SEY6210.1 *Trs130-mNeonGreen::HIS3 arf1Δ::KanMX*	This study
CFY2546	RSY298 *Trs130-mNeonGreen::HIS3*	This study
CFY2562	SEY6210 *Trs130-mNeonGreen-HA::TRP1 pik1Δ::HIS3 pik1-139* (plasmid)	This study
CFY2603	SEY6210.1 *Trs130-3xmRFPmars::TRP1*	This study
CFY2604	SEY6210.1 *Trs130-3xmRFPmars::TRP1 GFP-Vrg4*	This study
CFY2630	SEY6210.1 *Trs130-mNeonGreen::HIS3 Gea1-3xmRFPmars::TRP1*	This study
CFY2698	SEY6210 *Trs130-mNeonGreen::HIS3 Sec7-6xDsRed::URA3*	This study
CFY2701	SEY6210 *Trs130-mNeonGreen::HIS3 Sec7-mRFPmars::TRP1 erg6Δ::KanMX*	This study
CFY2710	SEY6210.1 *Trs130-3xmRFPmars::TRP1 GFP-hFAPP1 PH domain::URA3*	This study
CFY2743	BY4741α *Trs130-mNeonGreen::HIS3*	This study
CFY2745	BY4741α *Trs130-mNeonGreen::HIS3 drs2Δ::KanMX*	This study
CFY2801	SEY6210.1 *Trs130-3xmRFPmars::TRP1 GFP-Ypt31::URA3*	This study
CFY2803	SEY6210.1 *Trs130-3xmRFPmars::TRP1 GFP-Ypt32::URA3*	This study
CFY2818	SEY6210 *GFP-Ypt31::URA3 Sec7-mRFPmars::TRP1 erg6Δ::KanMX*	This study
CFY2821	SEY6210.1 *Trs130-3xmRFPmars::TRP1 gyp1Δ::KanMX*	This study

Table S3. **Liposome formulations used in this study.**

Lipid	TGN complete	TGN anionic	TGN neutral	PC
	%	%	%	%
DOPC	24	57	60	99
POPC	6	6	6	-
DOPE	7	-	7	-
POPE	3	-	3	-
DOPS	1	1	-	-
POPS	2	2	-	-
DOPA	1	1	-	-
POPA	2	2	-	-
PI	29	29	-	-
PI(4)P	1	1	-	-
CDP-DAG	2	-	2	-
DO-DAG	2	-	2	-
PO-DAG	4	-	4	-
Ceramide (C18)	5	-	5	-
Cholesterol	10	-	10	-
DiR dye	1	1	1	1

-, NA; CDP-DAG, 1,2-dipalmitoyl-*sn*-glycero-3-cytidine diphosphate; DiR, near-infrared dye; DO-DAG, 1,2-dioleoyl-*sn*-glycerol; DOPA; 1,2-dioleoyl-*sn*-glycero-3-phosphate; DOPC, 1,2-dioleoyl-*sn*-glycero-3-phosphocholine; DOPE, 1,2-dioleoyl-*sn*-glycero-3-phosphoethanolamine; DOPS, 1,2-dioleoyl-*sn*-glycero-3-phospho-L-serine; PO-DAG, 1-palmitoyl-2-oleoyl-*sn*-glycerol; POPA, 1-palmitoyl-2-oleoyl-*sn*-glycero-3-phosphate; POPC, 1-palmitoyl-2-oleoyl-*sn*-glycero-3-phosphocholine; POPE, 1-palmitoyl-2-oleoyl-*sn*-glycero-3-phosphoethanolamine; POPS, 1-palmitoyl-2-oleoyl-*sn*-glycero-3-phospho-L-serine.

References

Brachmann, C.B., A. Davies, G.J. Cost, E. Caputo, J. Li, P. Hieter, and J.D. Boeke. 1998. Designer deletion strains derived from *Saccharomyces cerevisiae* S288C: a useful set of strains and plasmids for PCR-mediated gene disruption and other applications. *Yeast.* 14:115–132. http://dx.doi.org/10.1002/(SICI)1097-0061(19980130)14:2<115::AID-YEA204>3.0.CO;2-2

Buvelot Frei, S., P.B. Rahl, M. Nussbaum, B.J. Briggs, M. Calero, S. Janeczko, A.D. Regan, C.Z. Chen, Y. Barral, G.R. Whittaker, and R.N. Collins. 2006. Bioinformatic and comparative localization of Rab proteins reveals functional insights into the uncharacterized GTPases Ypt10p and Ypt11p. *Mol. Cell. Biol.* 26:7299–7317. http://dx.doi.org/10.1128/MCB.02405-05

Duronio, R.J., E. Jackson-Machelski, R.O. Heuckeroth, P.O. Olins, C.S. Devine, W. Yonemoto, L.W. Slice, S.S. Taylor, and J.I. Gordon. 1990. Protein N-myristoylation in *Escherichia coli*: Reconstitution of a eukaryotic protein modification in bacteria. *Proc. Natl. Acad. Sci. USA.* 87:1506–1510. http://dx.doi.org/10.1073/pnas.87.4.1506

Esmon, B., P. Novick, and R. Schekman. 1981. Compartmentalized assembly of oligosaccharides on exported glycoproteins in yeast. *Cell.* 25:451–460. http://dx.doi.org/10.1016/0092-8674(81)90063-5

Goody, R.S., A. Rak, and K. Alexandrov. 2005. The structural and mechanistic basis for recycling of Rab proteins between membrane compartments. *Cell. Mol. Life Sci.* 62:1657–1670. http://dx.doi.org/10.1007/s00018-005-4486-8

Levine, T.P., and S. Munro. 2002. Targeting of Golgi-specific pleckstrin homology domains involves both PtdIns 4-kinase-dependent and -independent components. *Curr. Biol.* 12:695–704. http://dx.doi.org/10.1016/S0960-9822(02)00779-0

Lewis, M.J., B.J. Nichols, C. Prescianotto-Baschong, H. Riezman, and H.R. Pelham. 2000. Specific retrieval of the exocytic SNARE Snc1p from early yeast endosomes. *Mol. Biol. Cell.* 11:23–38. http://dx.doi.org/10.1091/mbc.11.1.23

Losev, E., C.A. Reinke, J. Jellen, D.E. Strongin, B.J. Bevis, and B.S. Glick. 2006. Golgi maturation visualized in living yeast. *Nature.* 441:1002–1006. http://dx.doi.org/10.1038/nature04717

McDonold, C.M., and J.C. Fromme. 2014. Four GTPases differentially regulate the Sec7 Arf-GEF to direct traffic at the trans-golgi network. *Dev. Cell.* 30:759–767. http://dx.doi.org/10.1016/j.devcel.2014.07.016

Robinson, J.S., D.J. Klionsky, L.M. Banta, and S.D. Emr. 1988. Protein sorting in *Saccharomyces cerevisiae*: Isolation of mutants defective in the delivery and processing of multiple vacuolar hydrolases. *Mol. Cell. Biol.* 8:4936–4948. http://dx.doi.org/10.1128/MCB.8.11.4936

Sciorra, V.A., A. Audhya, A.B. Parsons, N. Segev, C. Boone, and S.D. Emr. 2005. Synthetic genetic array analysis of the PtdIns 4-kinase Pik1p identifies components in a Golgi-specific Ypt31/rab-GTPase signaling pathway. *Mol. Biol. Cell.* 16:776–793. http://dx.doi.org/10.1091/mbc.E04-08-0700

Sikorski, R.S., and P. Hieter. 1989. A system of shuttle vectors and yeast host strains designed for efficient manipulation of DNA in *Saccharomyces cerevisiae*. *Genetics.* 122:19–27.

Weiss, O., J. Holden, C. Rulka, and R.A. Kahn. 1989. Nucleotide binding and cofactor activities of purified bovine brain and bacterially expressed ADP-ribosylation factor. *J. Biol. Chem.* 264:21066–21072.